Reexamination of high-energy above-threshold ionization (ATI): An alternative strong-field ATI model

V. I. Usachenko* and V. A. Pazdzersky
Institute of Applied Laser Physics of Uzbekistan Academy of Sciences, Nakashlyk Street 1, Tashkent 700185, Uzbekistan and Physics Department of National University of Uzbekistan, Vuzgorodok, Tashkent 700174, Uzbekistan

J. K. McIver
Center for Advanced Studies and Department of Physics and Astronomy, University of New Mexico, Albuquerque, New Mexico 87131, USA

(Received 26 May 2002; revised manuscript received 4 November 2003; published 21 January 2004)

The multiphoton strong-field phenomenon of high-energy above-threshold ionization (or high-order ATI) of an isolated atomic system exposed to an intense monochromatic linearly polarized laser field is considered analytically and studied numerically within the framework of an alternative nonrelativistic strong-field approach developed earlier for theoretical treatment of high-order harmonic generation process. The related proposed alternative strong-field ATI model is fully quantum mechanical and mainly based on the *Keldysh approximation* combined with making use of the *essential states* method (along with the *pole approximation*). Applying together these two methods allows for representation of the total ATI amplitude in a closed and compact analytical (the so-called *factorized*) form quite transparent for interpretation and available for direct numerical calculations. To demonstrate the model applicability, a number of certain photoelectron spectra produced by various atomic species (mostly noble gas atoms and negative ions) have been calculated numerically and shown to reproduce the well-known conventional semiclassical rule for the extent of high-energy plateau and position of its cutoff energy. All the calculated photoelectron spectra as well as the specific details of respective angular distributions (viz., their sidelobes or so-called *rings*) corresponding to a certain photoelectron peak within a high-energy plateau region (formed primarily by *rescattered* photoelectrons) demonstrate a very credible behavior within a broad and most interesting region of the problem parameters. Moreover, they all are also in an excellent or fairly good accordance with typical ones measured in standard ATI experiments or calculated by other authors within different (analytically more sophisticated or computationally very demanding) approaches and methods developed earlier.

DOI: 10.1103/PhysRevA.69.013406 PACS number(s): 32.80.Rm, 32.80.Fb

I. INTRODUCTION

The above-threshold ionization (ATI) process in atomic, molecular, and other systems exposed to an intense electromagnetic (em) laser field is probably the most fundamental and intriguing strong-field phenomenon of modern strong-field atomic, molecular, and optical (AMO) physics. Due to various possible related promising applications, this phenomenon attracted a lot of theoretical and experimental attention during the last two decades [1,2]. Currently, the ATI process is commonly recognized as an essentially multiphoton process along the course of which the laser-irradiated system (atom, molecule, etc.) absorbs a number N of incident photons of fundamental frequency ω well over the minimal one N_0 required to overcome the ionization potential I_p ($N > N_0 = [I_p/\omega] + 1 \gg 1$, here $[x]$ denotes an integer part of variable x and the *atomic system of units* is used throughout this paper unless stated otherwise). The underlying physical mechanism, initially identified as the *direct ATI process* [3], is related to the fact that, prior to final escaping, the optical atomic electron, being released to atomic continuum states, is still under the influence of the atomic binding potential and, therefore, able to absorb a number of additional (extra) photons of the incident laser radiation field. Accordingly, a typical ATI photoelectron spectrum is generally observed as a sequence of few equidistant peaks separated from each other by a fundamental laser frequency ω and corresponding to the number of extra photons absorbed. In the first experiments [4] (see also, e.g., Ref. [5] for review), the incident laser fields of relatively low or moderate intensity were mostly used and, therefore, the heights of these photoelectron peaks were found quickly dropping off with increasing photoelectron energy; however, more (additional) photoelectron peaks of higher energies were observed to appear with further increasing of the incident laser intensity. Soon after the first discovery and experimental observation, this phenomenon was realized and conceived as highly nonlinear, particularly, this phenomenon can not be described yet by any finite-order perturbation theory with respect to em interaction with the incident laser field of very high intensity [1,5]. Furthermore, beginning from a critical value of laser intensity $I > I_c$ (so that $U_p \geqslant \omega$, here U_p is the ponderomotive energy or cycle-averaged kinetic energy of oscillating motion of a free electron driven by an incident laser field only) the nonperturbative character of ATI process becomes especially obvious and prominent. Particularly, in a laser radiation field of very high intensity a few lowest-energy photoelectron peaks (i.e., corresponding to several least net num-

*Author to whom correspondence should be addressed. Email address: vusach@yahoo.com

 ©2004 The American Physical Society

bers of incident photons absorbed to overcome the ionization threshold) were found to have considerably smaller heights (or even be highly suppressed) compared to peaks of higher energies corresponding to a larger number of absorbed photons (the so-called *strong-field suppression* of low-energy ATI peaks [5]).

In this context, the process of *high-energy above-threshold ionization* (HATI) is a strong-field phenomenon of much higher order of nonlinearity corresponding to a much larger net number of incident photons absorbed, so that, eventually, the laser-irradiated system is able to produce considerably faster photoelectrons of energy $\varepsilon_p > 2U_p \gg \omega$, i.e., far beyond the conventional energy region where the direct ATI process is predominant. A highly nonperturbative nature of the HATI process becomes especially distinct and manifest, in particular, by existence of so-called *high-energy plateau* in high-energy photoelectron spectra [6,7] and anomalous angular distributions (viz., sidelobes or so-called *rings* [8]) of faster photoelectrons revealed in experiments. Since then the HATI process became the subject of a great number of theoretical and experimental studies (see, e.g., Refs. [9–11] for reviews). Such an intensive and explosive interest is mostly fundamental due to the fact that high-precision experiments on single atoms are feasible, which allow for a detailed comparison between experiment and theory, in contrast with other related strong-field phenomenon of high-order harmonic generation (HHG) whose analysis is impeded by the existence of collective and propagation effects. Owing to these investigations undertaken in the past ten years, it was ascertained that typically produced high-energy photoelectron spectra observed in ATI experiments demonstrate the similar universal generic behavior, despite a number of particular differences in shape and detailed structure: namely, they can be distinctly split into three different regions of photoelectron energy: (i) $\varepsilon_p \leqslant 2U_p$, where the heights of photoelectron peaks variate and generally fall down, (ii) $2U_p \leqslant \varepsilon_p \leqslant 10U_p$, the so-called plateau region where the heights of photoelectron peaks are of about the same order, (iii) after plateau cutoff energy region $\varepsilon_p > \varepsilon_{cutoff} \approx 10U_p$, where the produced photoelectron peaks demonstrate quickly decreasing heights and, finally, exhibit a negligibly small intensity.

Presently, there are two different principal approaches to theoretical treatment of the ATI process and all the existing, developed, and currently applied theoretical models and methods can be accordingly divided into two main groups. The first one is based on pure numerical procedures and methods, such as the direct numerical integration of one-dimensional (1D) (e.g., Refs. [1,12]) or 3D time-dependent Schrödinger equation (TDSE, e.g., Ref. [13], see also Refs. [10,11] for recent progress), time-dependent density-functional theory approach (e.g., Ref. [14]) or the Floquet calculations (e.g., Refs. [15,16]). Although these *ab initio* numerical approaches (see also Ref. [17]) are the most straightforward and have a valuable advantage that there are no restrictions to be imposed on the type of the incident laser pulse (so that the respective numerical solutions can, in principle, be obtained for all regimes of incident field intensity and frequency), nonetheless, their results are computationally very demanding and hardly available for transparent interpretation. The second approach (see, e.g., Refs. [18–26]) is based on the conventional strong-field approximation (SFA) applied within standard single-active-electron (SAE) *S*-matrix formalism. Excluding very rare exceptions (e.g., Refs. [21,24]), this approach generally implies also a substantial exploiting of the steepest descend (or *saddle-point*) method under related analytical calculations of the quantum-mechanical amplitude of the rescattering ATI process and/or interpretation of final numerical results. Therefore, the latter mentioned ATI models are essentially formulated in terms of a quantum-mechanical path integral which, due to the applied saddle-point method, can be approximately constructed from the classical orbits of a released electron driven by the incident laser field. Only for this reason, these strong-field ATI models can be conditionally referred further as *quasiclassical* ones due to the associated semiclassical analysis of the most contributing classical orbits (''pathways'') of the released electron in intermediate continuum states (so-called *quantum paths*) that makes the latter ATI models quite conceivable intuitively. In the meanwhile, the underlying semiclassical analysis goes back to the well-known classical (the so-called *two-step simple-man*) ATI model that was, historically, the simplest version of completely classical consideration of strong-field processes (see, e.g., Ref. [27] and relevant references cited therein) and improved later by means of taking the rescattering of the released electron into account (the so-called *three-step simple-man* model [28]). In particular, according to the three-step simple-man model, the origin of the high-energy photoelectron plateau was identified and explained as directly related to the initial release of an active (optical) electron followed by a possible (completely classical) return back to the site of release and final rescattering off the parent core. During the course of rescattering the returning electron undergoes a considerable additional acceleration by the incident field and, thereby, acquires a significant additional energy (much higher than without this rescattering event) and, only afterwards, it escapes eventually as a high-energy photoelectron. This completely classical picture of the so-called rescattering ATI process was later improved by tunneling, dispersion, etc., taking into more or less exact account (e.g., Refs. [29,30]). Therefore, these latter versions (primarily classical ATI models) will be referred further (also, just for brevity) as *semiclassical* or simple-man-based models, unlike previously mentioned *quasiclassical* (though, primarily quantum-mechanical SFA-based) ATI models. Thus, according to any SFA-based quasiclassical or simple-man-based semiclassical model cited above and their diverse modifications (the listing of related references is inevitably incomplete), the cutoff energy of high-energy plateau in the photoelectron spectrum is associated with the largest possible value of kinetic energy acquired by the released electron from driving laser field owing to the final rescattering (backscattering) off the parent core. However, the applying of the saddle-point method along with essential exploiting of this completely classical underlying picture seems to be quite inconvenient in a number of particular cases (although, very important and promising for various practical applications) of incident laser fields of more

complex (nonstandard) frequency and polarization composition. For example, for two-color (bichromatic) laser field of arbitrary spatial and polarization compositions, the classical trajectories of the released electron driven by an incident two-color field are generally too overcomplicated [31]. This makes the respective underlying transcendental equation of classical motion a considerably less compliant to the related fully 3D numerical analysis for finding out all predominantly contributing classical trajectories. Due to a very sophisticated and too cumbersome numerical computation procedure (e.g., Ref. [32]) such an analysis seems to be reliably possible only for the simplest two-color laser field configurations [32–34]. Nonetheless, for a particular case of the model zero-range potential (ZRP) frequently used for approximate description of the atomic binding potential, the saddle-point method and associated semiclassical analysis were shown to be quite avoidable within a different (neither semiclassical nor quasiclassical, but exact) SFA-based quantum-mechanical approach [21,24] developed previously (see also Ref. [35]), although at the expense of its restricted applicability to ZRP-bound laser-irradiated systems only.

In our opinion, such a situation can hardly be considered as quite satisfactory. This gave some reasonable justification and a strong primary motivation for the present paper in which we attempt to revisit the high-energy ATI process in the framework of quite a different, though also nonrelativistic, fully quantum-mechanical strong-field approach proposed earlier [36] and applied first to the HHG process in isolated laser-exposed atomic systems for effective numerical calculation of associated HHG spectra. Just as the most of previously developed strong-field analytical models (e.g., quasiclassical ones mentioned above), the currently developed ATI model is also based mainly on the strong-field approximation (well applicable for large values of the Reiss parameter [37] $\eta = U_p/\omega \gg 1$). Therefore, the model also describes the strong-field ionization process in terms of nonperturbative SAE atomic response consisting of a superposition of two highly nonlinear processes of emission of lower-energy electrons (due to the direct ATI process) of energies up to about $2U_p - 2.5U_p$ and higher-energy electrons (due to the rescattering ATI process) of energies up to $10U_p$. However, unlike semiclassical or quasiclassical SFA-based ATI models mentioned above, the underlying *alternative* strong-field approach incorporates also quite a different, the so-called *essential states* method [38] and the associated *pole approximation* (see also Ref. [39], for details as well as the relevant references cited therein). Thus, the currently applied strong-field approach is developed entirely beyond any semiclassical (though, attractive and very beautiful) concept of the most contributing classical trajectories (or *quantum paths*) of a released electron in intermediate continuum states. Nonetheless, the derived analytical expressions are also quite conceivable and transparent for interpretation; moreover, they seem to have been derived in a more straightforward way that does not imply any further numerical analysis of the underlying transcendental equation corresponding to completely classical return of the released electron back to the site of its release and subsequent finding out and thorough selection of only those trajectories that are predominantly contributing to the SFA amplitude of the photoprocess under consideration. The latter means that the corresponding final results (the calculated ATI spectra) are obtained without any intensive computation work needed within other (often more analytically sophisticated) approaches and methods developed earlier. This also means that, without any serious analytical restrictions or numerical complications, the final analytical expressions derived for total ionization rates and associated photoelectron angular distributions can be equally well extended to more general cases of two-color incident laser fields. In the meantime, two-color strong-field phenomena due to em interaction with bichromatic laser field are currently believed to be highly promising for a number of numerous fascinating applications, e.g., related to the so-called *coherent control* the detailed properties of two-color multiphoton process that might provide a principal possibility of manipulating (engineering) the associated spectra (see, e.g., Ref. [40] for a review). At last, although the high-energy ATI process has proven to produce highly structured spectra, nevertheless, the presented ATI model is able to adequately describe both a general shape and even the details of a fine structure of high-energy photoelectron spectra as well as their nonlinear behavior within the most interesting region of the problem parameters provided the condition of nonrelativistic treatment of the problem is still satisfied. As follows from the results of our numerical calculations presented in Sec. IV, all the high-energy photoelectron spectra calculated and presented here are to a fairly good accuracy consistent with respective results of different strong-field approaches developed earlier by other authors or measured in relevant experiments. Particularly, all the results presented here also well reproduce the conventional semiclassical rule "$\varepsilon_{cutoff} \approx 10U_p$" for the high-energy plateau cutoff and adequately describe the associated specific anomalous angular photoelectron distributions (viz., the sidelobes or rings) formed primarily by high-energy (or rescattered) photoelectrons.

II. GENERAL SFA FORMALISM AND BACKGROUND THEORY OF ATI MODEL

Just as the most of previously developed strong-field Keldysh-Faisal-Reiss (KFR)-based models, our present consideration of the high-energy ATI process is restricted to nonrelativistic frameworks traditionally supposing the photoelectron kinetic energy $\varepsilon = v^2/2$ and the ponderomotive energy U_p (the energy of oscillating motion of a free electron driven by incident laser field) are both negligibly small as compared to the electron rest energy ($v^2 \ll c_0^2$, $U_p \ll c_0^2$, $c_0 \approx 137$ is the light velocity in vacuum). The latter means that, with a fairly good accuracy, the em interaction of an active (optical) electron with a strong driving laser field can be considered within the *dipole* (or, *long-wavelength*) *approximation* (neglecting any photon momenta, $\mathbf{k}=0$) wherein the incident field strength $\mathbf{E}(t)$ and associated vector potential $\mathbf{A}(t)$ are independent on coordinate radius vector $\mathbf{r}$, but both are functions of time t only. Hence, the respective Hamiltonian of em interaction of the electron with incident laser

field may be written, for example, in $(\mathbf{A}\cdot\mathbf{p})$ (the so-called "*velocity*" gauge) form:

$$\hat{W}(\mathbf{r},t)=\frac{1}{c_0}\mathbf{A}(t)\cdot\hat{\mathbf{p}}+\frac{1}{2c_0^2}\mathbf{A}^2(t), \tag{1}$$

here $\hat{\mathbf{p}}=-i\boldsymbol{\nabla}$ is the operator of electron canonical momentum.

Owing to a very high intensity the incident laser field can be described within completely classical frameworks wherein the explicit form of its vector potential $\mathbf{A}(t)$ is given by the following conventional expression:

$$\mathbf{A}(t)=(c_0/\omega)\mathbf{e}E\cos(\omega t), \tag{2}$$

where $\mathbf{e}$ and E are the unit polarization vector and electric field strength, respectively. Then, the motion of a free electron driven by field (2) is described by the well-known *Volkov's wave function* that is just an *exact solution* of the time-dependent Schrödinger equation with the Hamiltonian $H_F=\hat{\mathbf{p}}^2/2+\hat{W}(\mathbf{r},t)$. The explicit nonrelativistic expression for this solution corresponding to continuous spectrum states of a definite value of electron canonical momentum $\mathbf{p}$ reads as (e.g., Ref. [41])

$$\psi_{\mathbf{p}}(\mathbf{r},t)=(2\pi)^{-3/2}\exp\left[i(\mathbf{p}\cdot\mathbf{r})-\frac{i}{2}\int_{-\infty}^{t}\left(\mathbf{p}+\frac{1}{c_0}\mathbf{A}(t')\right)^2dt'\right]. \tag{3}$$

For the particular case of linearly polarized monochromatic incident field (2) the expression for nonrelativistic Volkov's wave function (3) can be also represented in the form of expansion in harmonics of laser field frequency ω [37,41]:

$$\psi_{\mathbf{p}}(\mathbf{r},t)=|\mathbf{p}\rangle\times\sum_{s=-\infty}^{\infty}B_s\left(\zeta(\mathbf{p});\frac{\eta}{2}\right)\exp\left[-i\left(\frac{\mathbf{p}^2}{2}+U_p+s\omega\right)t\right], \tag{4}$$

i.e., in terms of electron plane wave functions $|\mathbf{p}\rangle$ and the generalized Bessel function of the first kind and s th order,

$$B_s(x;y)=\sum_{m=-\infty}^{\infty}J_{s-2m}(x)J_m(y), \tag{5}$$

and of two real arguments, where $J_s(x)$ is an ordinary s-th-order Bessel function of the first kind and real argument x; moreover, the two dimensionless parameters $\zeta(\mathbf{p})=(\mathbf{E}\cdot\mathbf{p})/\omega^2$ and $\eta=U_p/\omega=E^2/(4\omega^3)$ (the latter is also known as *the Reiss parameter* [37,42]) have been additionally introduced here.

Let us start by introducing a total wave function $\Psi(\mathbf{r},t)$ as an exact solution of the total nonstationary Schrödinger equation:

$$i\frac{\partial}{\partial t}\Psi(\mathbf{r},t)=\hat{H}\Psi(\mathbf{r},t)=\{\hat{T}+\hat{V}(\mathbf{r})+\hat{W}(\mathbf{r},t)\}\Psi(\mathbf{r},t) \tag{6}$$

for the considered laser-irradiated system *dressed* by the incident strong laser em field (2). Here $\hat{T}=-\frac{1}{2}\boldsymbol{\nabla}^2$ is the operator of an active electron kinetic energy, $\hat{V}(\mathbf{r})$ is the operator of electron interaction with a residual parent core, so that the SAE approximation is supposed to be applicable: namely, only one of the electrons [the so-called optical electron moving in the averaged "*effective*" binding potential $V(\mathbf{r})$ screened by the time-independent charge distribution of all remaining "*inactive*" electrons] is allowed to respond to the incident laser field. After making a conventional supposition about adiabatic turning on and off any electron-photon em interaction at extremely long interaction time ($t\rightarrow\pm\infty$) the nonstationary Schrödinger equation (6) can be rewritten in the following equivalent integral form:

$$\Psi_{out}^{(-)}(\mathbf{r},t)=\psi_{\mathbf{p}}(\mathbf{r},t)+\int_t^{\infty}dt'\int G^{(-)}(\mathbf{r},t;\mathbf{r}',t')\times\hat{V}(\mathbf{r}')\psi_{\mathbf{p}}(\mathbf{r}',t')d\mathbf{r}' \tag{7}$$

corresponding to different initial- and final-time conditions for the ATI process and the latter equation seems to be more convenient for further consideration. The operator $G^{(\pm)}(\mathbf{r},t;\mathbf{r}',t')$ of time evolution introduced here is just the total propagator, i.e., either *the total advanced* $[G^{(-)}(\mathbf{r},t;\mathbf{r}',t')=0$ at $t>t']$ or retarded $[G^{(+)}(\mathbf{r},t;\mathbf{r}',t')=0$ at $t<t']$ *Green function* corresponding to the exact solution of the total nonstationary Schrödinger equation (6) with two strong interactions $\hat{W}(\mathbf{r},t)$ and $\hat{V}(\mathbf{r})$ of comparable strength taken into exact account.

According to a general S-matrix formalism of SFA approach (see, e.g., Refs. [37,42]), the time-independent amplitude of the ATI process can be, particularly, represented via the standard matrix element of the em interaction (1):

$$F_{i\rightarrow f}^{(ATI)}(\mathbf{p})=-i\lim_{T\rightarrow-\infty}\int_T^{\infty}dt\int d\mathbf{r}\langle\Psi_{out}^{(-)}(\mathbf{r},t)\times|\hat{W}(\mathbf{r},t)|\Phi_0(\mathbf{r},t)\rangle, \tag{8}$$

i.e., via S matrix of em transition from the "initial" bound discrete state $\Phi_0(\mathbf{r},t)=\Phi_0(\mathbf{r})\cdot\exp(-i\varepsilon_0 t)$ (here $|\varepsilon_0|=I_p$ is the ionization potential) of the unperturbed laser-exposed system (with no em field present) to the field-perturbed "final" out-state $\Psi_{out}^{(-)}(\mathbf{r},t)$ corresponding to the wave function of continuous spectrum states of the ionized laser-exposed system dressed by the incident laser field and containing the complete effects of the incident field and the binding potential. Thus, the total ATI amplitude (8) is written in terms of expansion in the interaction $\hat{W}(\mathbf{r},t)$ and corresponds to taking this interaction into account only in a final state dressed by the incident strong laser field (see also Refs. [37,42] for an extent listing of various possible representations of S matrices and respective SFA amplitudes). After substituting Eq. (7) in Eq. (8), the latter expression for the total ATI amplitude takes the form

$$F_{i\rightarrow f}^{(ATI)}(\mathbf{p})=F_{i\rightarrow f}^{(DATI)}(\mathbf{p})+F_{i\rightarrow f}^{(RATI)}(\mathbf{p}). \tag{9}$$

Here the first term in the right-hand side,

$$F_{i\to f}^{(DATI)}(\mathbf{p}) = -i\int_{-\infty}^{\infty} dt\langle \psi_{\mathbf{p}}(\mathbf{r},t)|\hat{W}(\mathbf{r},t)|\Phi_0(\mathbf{r},t)\rangle, \tag{10}$$

is just a general expression for the amplitude of the direct ATI process derived within the standard *Keldysh approximation* [43], whereas the second term

$$F_{i\to f}^{(RATI)}(\mathbf{p}) = -i\int_{-\infty}^{\infty} dt \int d\mathbf{r}\psi_{\mathbf{p}}^{*}(\mathbf{r},t)\hat{V}(\mathbf{r}) \times \int_{-\infty}^{t} dt' \int d\mathbf{r}' G^{(+)}(\mathbf{r},t;\mathbf{r}',t')\hat{W}(\mathbf{r}',t') \times \Phi_0(\mathbf{r}',t') \tag{11}$$

corresponds to the SFA amplitude of the so-called rescattering ATI process (or emission of a high-energy photoelectron).

By means of substitution of the explicit expression for Volkov's function (4) in Eq. (10) and elementary analytical integration over the time variable (just resulting the singular Dirac δ function which provides the conservation of total energy in the process), amplitude (10) of the direct ATI process can be represented in the following conventional form:

$$F_{i\to f}^{(DATI)}(\mathbf{p}) \approx 2\pi \sum_{N=-\infty}^{\infty} f_{DATI}^{(N)}(\mathbf{p},\eta)\,\delta(\varepsilon_{\mathbf{p}} + I_p + U_p - N\omega) \tag{12}$$

that is the well-known expression derived within standard KFR theories [43]. Here each Nth item of infinite sum in Eq. (12) corresponds to the respective partial (of Nth order) amplitude of the direct ATI process:

$$f_{DATI}^{(N)}(\mathbf{p},\eta) = -i\Phi_0(\mathbf{p})(U_p - N\omega)B_{-N}\left(\zeta(\mathbf{p});\frac{\eta}{2}\right) \tag{13}$$

defining the probability for the laser-exposed system to absorb N incident photons and produce a photoelectron of the energy $\varepsilon_{\mathbf{p}}^{(N)} = \mathbf{p}_N^2/2 = N\omega - I_p - U_p$ due to the direct ATI process only. Whereas

$$\Phi_0(\mathbf{p}) = \langle \mathbf{p}|\Phi_0(\mathbf{r})\rangle = (2\pi)^{-3/2}\int d\mathbf{r}\exp[-i(\mathbf{p}\cdot\mathbf{r})]\Phi_0(\mathbf{r}) \tag{14}$$

is the Fourier transform of stationary wave function $\Phi_0(\mathbf{r})$ of the initial discrete state of the laser-irradiated (atomic) system.

Up to this point, no approximation was made nor any of the two strong interactions [$\hat{W}(\mathbf{r},t)$ or $\hat{V}(\mathbf{r})$] neglected or somehow discriminated, but only the underlying equations were just rewritten in a different form that seems to be more convenient for further consideration, so that all the previously presented expressions are still exact. From this point, we will follow further general concepts of the SFA approach (this is *the first main key approximation* made within the proposed strong-field approach and related ATI model) according to which, at any moment of time evolution, the laser-irradiated system is considered as being under action of only one of two strong interactions of comparable strength [i.e., either $W(\mathbf{r},t)$ or $V(\mathbf{r})$] separately, but never under both simultaneously. Such a presumption is quite conventional for various so-called KFR-based approaches [42] and, being applied to the treatment of any strong-field multiphoton process (such as, e.g., atomic photoionization), it corresponds, in fact, to neglecting the influence of the incident laser field on an initial atomic discrete state (for which the interaction with binding atomic potential is predominant) as well as neglecting the influence of the field of the residual parent core on the motion of the released electron in atomic continuum states (for which the em interaction with a strong driving laser field is predominant and, therefore, taken into account only). This approximation is valid mostly in the photoelectron energy region far away from the ionization threshold ($\varepsilon_{\mathbf{p}} = \mathbf{p}^2/2 \geqslant I_p \gg \omega$) where the influence of interaction with a parent residual atomic core is negligibly small. In the context of high-energy ATI process under consideration, the validity of SFA seems to be also sufficiently well justified (especially for the high-energy plateau region corresponding to a much higher energy of the ATI photoelectron $\varepsilon_{\mathbf{p}} \geqslant 2U_p \gg \omega$) owing to a very large net number $N > N_0 \gg 1$ of incident photons absorbed. For the total amplitude (8) of the high-energy ATI process under consideration, the applying of the SFA approach is just reduced, in fact, to the following approximate replacement:

$$G^{(+)}(\mathbf{r},t;\mathbf{r}',t') \approx G_V^{(+)}(\mathbf{r},t;\mathbf{r}',t') = -i\theta(t-t')\int \psi_{\mathbf{q}}(\mathbf{r},t)\psi_{\mathbf{q}}^{*}(\mathbf{r}',t')d\mathbf{q}, \tag{15}$$

where $\theta(t)$ is the Heaviside stepwise function and $G_V^{(+)}(\mathbf{r},t;\mathbf{r}',t')$ is just the retarded Volkov's Green function or nonrelativistic Volkov's propagator. Meanwhile, by direct substitution of Eq. (15) in Eq. (11) we arrive at the general SFA expression for the rescattering ATI amplitude:

$$F_{i\to f}^{(RATI)}(\mathbf{p}) = \int_{-\infty}^{\infty} dt \int d\mathbf{q}\langle \psi_{\mathbf{p}}(\mathbf{r},t)|\hat{V}(\mathbf{r})|\psi_{\mathbf{q}}(\mathbf{r},t)\rangle \times \int_{-\infty}^{t} dt'\langle \psi_{\mathbf{q}}(\mathbf{r},t')|\hat{W}(\mathbf{r},t')|\Phi_0(\mathbf{r},t')\rangle. \tag{16}$$

Just as amplitude (10) of the direct ATI process in which, after initial absorption of incident field photons and release from the initial (ground) state $\Phi_0(\mathbf{r},t)$, the released electron escapes eventually to final atomic continuum states $\psi_{\mathbf{p}}(\mathbf{r},t)$ with the canonical momentum $\mathbf{p}$ corresponding to lower-energy photoelectron, the expression (16) for the rescattering ATI amplitude also allows for quite transparent physical interpretation: namely, the ATI amplitude (16) suggests a different mechanism of photoionization process in which, after initial absorption of incident field photons [due to EM interaction $\hat{W}(r,t)$], an optical electron releases from the initial

(ground) state $\Phi_0(\mathbf{r},t)$ to intermediate continuum states described by respective Volkov's wave functions $\psi_{\mathbf{q}}(\mathbf{r},t)$. Afterwards, being still in the neighborhood of the parent core and driven further by the incident laser field only, the released electron returns to the site of release and rescatters off the parent core due to the interaction $\hat{V}(\mathbf{r})$ with a scattering (the atomic binding) potential. During the course of the rescattering process the released electron undergoes a considerable acceleration, making a transition from intermediate atomic continuum states of canonical momentum $\mathbf{q}$ to final continuum states $\psi_{\mathbf{p}}(r,t)$ of canonical momentum $\mathbf{p}$. Owing to the latter rescattering process, the released electron is able to absorb an additional number of incident field photons and escapes eventually with a considerably higher energy than without this rescattering event responsible for the origin of the high-energy plateau in the photoelectron spectrum.

Regarding this semiclassical interpretation, it is worth special noting here that, as in the above mentioned strong-field quasiclassical ATI models, the use of strong-field approximation in form (15) corresponds to taking into account *only one* (*the first*) *rescattering event* finished by final escaping of the rescattered electron and producing a high-energy plateau (see also Sec. IV). The latter statement becomes more transparent and quite conceivable as soon as the total nonstationary Schrödinger equation (6) for the exact solution of total retarded Green function $G^{(+)}(\mathbf{r},t;\mathbf{r}',t')$ is rewritten in the following equivalent integral form:

$$G^{(+)}(\mathbf{r},t;\mathbf{r}',t') = G_V^{(+)}(\mathbf{r},t;\mathbf{r}',t') + \int_{-\infty}^{t} dt'' \int d\mathbf{r}'' G_V^{(+)}(\mathbf{r},t;\mathbf{r}'',t'') \times \hat{V}(\mathbf{r}'') G^{(+)}(\mathbf{r}'',t'';\mathbf{r}',t'). \quad (17)$$

Then, after direct substitution of the above equation in Eq. (11), one can immediately see that the approximation (15) is equivalent, in fact, to retaining only the first term [corresponding to the zeroth order of expansion with respect to the binding/scattering potential $\hat{V}(\mathbf{r})$] in the right-hand side of equation (17) and neglecting the second (integral) part responsible for the multiple rescattering [due to interaction $\hat{V}(\mathbf{r})$]. Despite the multiple rescattering being also generally possible in principle during the course of the high-energy ATI process, it is always neglected both in the previously cited strong-field ATI models and the currently developed one. Strictly speaking, the latter multiple rescattering should be distinguished from multiple return (*revisiting*) of the released electron back to the parent core that is possible prior to the first rescattering event actually happens. Indeed, along the first revisiting, the released electron may not rescatter off the parent core at all, but escape again and, being driven repeatedly by incident laser field back to the site of release, can be rescattered by the parent core and only thereafter escape eventually. Thus, the first rescattering event is not generally equivalent just to the first return of the released electron back to the parent core as was implicitly presumed within earlier versions of semiclassical and quasiclassical strong-field ATI models, in which only one (viz., the first) revisiting event was initially taken into account. Meantime, the multiple revisiting of the released electron under discussion was later identified as the underlying physical mechanism responsible for a huge effect of resonancelike enhancement of the level (or averaged height) of the high-energy photoelectron plateau observed in recent ATI experiments [44] and remarkably reproduced theoretically first in Ref. [45] within the framework of the TDSE-based numerical approach. This effect was also confirmed in a number of later theoretical works [46] and, particularly, fairly well reproduced by previously developed quasiclassical strong-field ATI models, though improved later by a constructive interference of a larger number of longer classical orbits of the released electron corresponding to the multiple revisiting (but, no multiple rescattering) also taken into account. In this regard, let us just note that, being developed beyond any semiclassical concepts of the most contributing classical trajectories (quantum paths), the currently proposed ATI model should *ab initio* incorporate the above-mentioned effects due to taking all the actually contributing trajectories (and, particularly, corresponding to multiple revisiting) of the released electron into proper account, though, also before the first rescattering event only (see also Secs. III and IV below for details). However, it is hardly worthwhile to fall here into further detailed discussion of all these particular issues and related effects (including the so-called channel-closing effects [46] and quantum interference [47] in HHG and high-energy ATI as well as various two-color aspects of the problem mentioned in the Introduction) as this deserves special consideration elsewhere, probably, as a subject of our future publication.

III. THE SPECIFIC DETAILS OF THE STRONG-FIELD ATI MODEL AND FINAL ANALYTICAL RELATIONS

Expressions (10) and (16) are also the main basis and starting point of other strong-field (SFA-based) analytical quantum-mechanical approaches (including quasiclassical ones) developed earlier. Therefore, let us outline now the main distinctive features differentiating the proposed strong-field approach from any other mentioned above. By means of substitution of the explicit expression for Volkov's wave function (4) to Eq. (16) and performing elementary integration over the time variable t', one can derive

$$\int_{-\infty}^{t} dt' \langle \psi_{\mathbf{q}}(\mathbf{r}',t') | \hat{W}(\mathbf{r}',t') | \Phi_0(\mathbf{r}',t') \rangle = -i\Phi_0(\mathbf{q}) \sum_{m=-\infty}^{\infty} B_m(\zeta(\mathbf{q});\eta) \times \frac{\exp[i(\varepsilon_{\mathbf{q}}+U_p+I_p-m\omega)t]}{[\varepsilon_{\mathbf{q}}+U_p+I_p-m\omega]-i\epsilon}, \quad \epsilon \to 0. \quad (18)$$

The analytical integration over the variable $q=|\mathbf{q}|$ in Eq. (18) can be performed by means of the so-called *pole approximation* (and this is *the next, second essential key point* of the currently applied strong-field approach) according to which

$$\lim_{\epsilon\to 0}\int_0^\infty \frac{f(q)d\varepsilon_{\mathbf{q}}}{\varepsilon_{\mathbf{q}}+I_p+U_p-m\omega\mp i\epsilon} = \mathcal{P}\int_0^\infty \frac{f(q)d\varepsilon_{\mathbf{q}}}{\varepsilon_{\mathbf{q}}+I_p+U_p-m\omega} \pm i\pi f(q_m)\approx \pm i\pi f(q_m). \tag{19}$$

Here the symbol $\mathcal{P}$ before the integral denotes the main (or, in other words, principal) value of the corresponding integral and the variable $q_m=\sqrt{2(m\omega-I_p-U_p)}$ denoting the discrete values of photoelectron canonical momentum corresponding to intermediate continuous states has been also introduced. The latter pole approximation used is quite a common place within the so-called essential states method [38,39]) applied first under theoretical treatment of strong-field ionization processes including the direct ATI process (i.e., without taking any photoelectron rescattering into account). Since then, being also later applied in the theoretical study of other allied strong-field atomic phenomena (see, e.g., Refs. [1,39] and relevant references cited therein), this method also proved to be a powerful and effective tool of strong-field AMO physics. Although the essential states method was developed as primarily phenomenological approach, nonetheless, it was verified to be adequately well working and very fruitful under nonperturbative consideration of the direct ATI process within frameworks of completely quantum-mechanical concepts only (see also, e.g., Refs. [1,11]). The application of this method is equivalent, in fact, to the supposition that only the intermediate *resonance* continuum states of photoelectron energy

$$\varepsilon_{\mathbf{q}}^{(m)}=m\omega-I_p-U_p \tag{20}$$

(the so-called continuum essential states) give the main (predominant) contribution to relevant compound em dipole matrix elements of structure similar to Eq. (16). Thus, only the second, a singular part (proportional to the imaginary unit) of expression (19) is supposed to be quite sufficient for retaining in respective final expressions for amplitudes of the photoprocess under consideration. It should be noted here that, due to the pole approximation, the infinite sum (over m) in Eq. (18) is thereby replaced by the (also infinite) summation only over region $m\geqslant N_0$, where $N_0=[(I_p+U_p)/\omega]+1\geqslant 1$ is the minimum possible number of absorbed photons required for ionization in a very strong incident laser field (viz., when $U_p\geqslant\omega$). Thus, the incident strong laser field raises the ionization threshold by a value corresponding to the ponderomotive energy U_p, so that the least (minimum) number $N_0=N_0(\eta)\sim\eta$ of absorbed photons required for ionization is strongly dependent on the incident laser field intensity I. The latter means, in fact, the summation in Eq. (18) is reduced to the summation only over (formally, also infinite) number of direct open ATI channels, i.e., over atomic continuum states to which the process of direct ATI is also possible and, thus, only these channels are supposed to contribute predominantly to the amplitude of the high-energy ATI process under consideration.

The direct substitution of Eq. (18) in Eq. (16) and subsequent approximate analytical integration over intermediate electron energy $\varepsilon_{\mathbf{q}}$ [according to Eqs. (19) and (20)] make it possible to perform the final elementary analytical integration over time variable t. For an infinitely large time $t\to+\infty$, the latter time integration just results the Dirac singular δ function expressing the conservation of total energy in the quantum-mechanical process under consideration. Finally, the expression for time-independent rescattering ATI amplitude (16) takes the following approximate form:

$$F_{i\to f}^{(RATI)}(\mathbf{p})\approx 2\pi\sum_{N=-\infty}^{\infty} f_{RATI}^{(N)}(\mathbf{p},\eta)\,\delta(\varepsilon_{\mathbf{p}}+I_p+U_p-N\cdot\omega), \tag{21}$$

where each Nth item of summation corresponds to the respective partial (of Nth order) rescattering ATI amplitude

$$\begin{aligned} f_{RATI}^{(N)}(\mathbf{p},\eta) &= \sum_{m\geqslant N_0}\int dO_{\mathbf{q}_m} f_{rescat}^{(m-N)}(\mathbf{p}-\mathbf{q}_m,\eta) f_{MPI}^{(m)}(\mathbf{q}_m,\eta) \\ &= -i\pi\sum_{m\geqslant N_0} q_m(U_p-m\omega)\int dO_{\mathbf{q}_m} V(\mathbf{p}-\mathbf{q}_m) \\ &\quad\times J_{m-N}(\zeta(\mathbf{p}-\mathbf{q}_m))\Phi_0(\mathbf{q}_m)B_{-m}\left(\zeta(\mathbf{q}_m);\frac{\eta}{2}\right) \end{aligned} \tag{22}$$

contributing to Nth photoelectron peak of energy $\varepsilon_{\mathbf{p}}^{(N)}=N\omega-I_p-U_p$, whereas $V(\mathbf{p}-\mathbf{q})=\langle\mathbf{p}|\hat{V}(\mathbf{r})|\mathbf{q}\rangle$ is just the Fourier transform of atomic binding potential $\hat{V}(\mathbf{r})$ of the laser-irradiated atomic system and $dO_{\mathbf{q}}$ is the solid angle element directed along the intermediate photoelectron canonical momentum $\mathbf{q}$.

As one can see from Eq. (22), the applied pole approximation also allows for representation of rescattering ATI amplitude (16) in the so-called factorized form that makes it quite transparent for interpretation. Particularly, within the framework of the currently developed strong-field ATI model, the rescattering ATI amplitude (22) is represented as a production of the time-independent amplitude:

$$f_{MPI}^{(m)}(\mathbf{q}_m)\sim -i\pi(U_p-n\omega)B_{-m}\left(\zeta(\mathbf{q}_m);\frac{\eta}{2}\right)\Phi_0(\mathbf{q}_m) \tag{23}$$

of direct multiquantum ionization (viz., accompanied by absorption of m incident field photons) of the initial atomic ground state $\Phi_0(\mathbf{r})$ to intermediate continuum states with the canonical momentum $q_m=\sqrt{2\varepsilon_{\mathbf{q}}^{(m)}}$ and the time-independent amplitude

$$f_{scat}^{(m-N)}(\mathbf{p}-\mathbf{q}_m,\eta)\sim -iq_m V(\mathbf{p}-\mathbf{q}_m)J_{m-N}(\zeta(\mathbf{p}-\mathbf{q}_m)) \tag{24}$$

of the subsequent process of laser-assisted scattering (rescattering) of the released electron off the parent core and transition of the laser-exposed system from intermediate continuum states (with the canonical momentum $\mathbf{q}_m$) to final

continuum states (with the canonical momentum **p**) accompanied by absorption or emission of an additional number of incident photons. Thus, just as in strong-field quasiclassical ATI models, there is also close and transparent interrelation between the direct and rescattering ATI processes, so that the possibility of the latter one is necessarily conditioned by an existence of the former one. It is also worth specially noting here (see also Ref. [39] for details) that the origin and nature of the currently discussed factorization of the rescattering ATI amplitude (24) are quite different from the similar (but more sophisticated) procedure of the so-called factorization technique proposed first in Ref. [48] and applied under theoretical treatment of atomic multiple (particularly, the so-called *nonsequential*) photoionization. The latter procedure was further extended to consideration of HHG and high-energy ATI processes within the framework of a different quantum-mechanical (though, also quasiclassical) strong-field approach (the so-called *atomic antenna* mechanism, see also Refs. [49,50]).

It is also well seen that the presence of singular Dirac δ function in the right-hand side of Eq. (21) makes the energy $\varepsilon_{\mathbf{p}}$ of the emitted photoelectron take only discrete values $\varepsilon_{\mathbf{p}} = \varepsilon_{\mathbf{p}}^{(N)}$ determined by Eq. (20) and separated from each other by the incident laser fundamental frequency ω. Consequently, within the proposed strong-field ATI model the produced photoelectron spectrum is also represented by a sequence of peaks of discrete energies $\varepsilon_{\mathbf{p}}^{(N)}$ and respective heights (peak intensities) determined by corresponding partial (of Nth order) ATI amplitudes:

$$f_{ATI}^{(N)}(\mathbf{p},\eta) = \{f_{DATI}^{(N)}(\mathbf{p},\eta) + f_{RATI}^{(N)}(\mathbf{p},\eta)\} \times \delta(\varepsilon_{\mathbf{p}} + I_p + U_p - N\omega) \tag{25}$$

in which the partial direct ATI amplitude $f_{DATI}^{(N)}(\mathbf{p},\eta)$ and rescattering ATI amplitude $f_{RATI}^{(N)}(\mathbf{p},\eta)$ are given by expressions (13) and (22), respectively. The respective partial differential ionization rates $w_{ATI}^{(N)}(\mathbf{p}_N)$ to absorb N incident photons and emit the photoelectron of the final momentum $p_N = \sqrt{2[N\omega - I_p - U_p]}$ to a fixed spatial direction along the solid angle element $dO_{\mathbf{p}_N}$ are conventionally found by means of a standard procedure of squaring module of total ATI amplitude (25) divided by a long normalization time and then integrated over the entire phase-space volume of emitted photoelectron final states:

$$w_{ATI}^{(N)}(\mathbf{p}_N,\eta) = \frac{dR_{ATI}^{(N)}(p_N,\eta)}{dO_{\mathbf{p}_N}} = \frac{p_N}{(2\pi)^2}\left|f_{DATI}^{(N)}(\mathbf{p}_N,\eta) + f_{RATI}^{(N)}(\mathbf{p}_N,\eta)\right|^2. \tag{26}$$

The ionization rates $R_{ATI}^{(N)}(p_N,\eta)$ introduced in Eq. (26) determine the respective *integral photoelectron spectrum* and they are found from Eq. (26) by integration of partial differential rates $w_{ATI}^{(N)}(\mathbf{p}_N,\eta)$ over all angles of photoelectron emission. Meanwhile, the partial differential rates (26) determine the produced photoelectron spectrum observed along the fixed direction of photoelectron emission (e.g., with respect to the direction of incident field polarization **e**) as well as the respective partial photoelectron angular distributions (PAD) corresponding to a fixed number N of photons absorbed. The total PAD $P_{ATI}^{(int)}(\mathbf{p},\eta)$ produced by all emitted photoelectrons can be found directly from Eq. (26) by means of summation over all contributing photoelectron peaks (or so-called open ATI channels each corresponding to a fixed final photoelectron energy $\varepsilon_{\mathbf{p}}^{(N)}$ in continuum states):

$$P_{ATI}^{(int)}(\theta,\eta) = \sum_{N=N_0}^{\infty} w_{ATI}^{(N)}(\mathbf{p}_N,\eta) = (2\pi)^{-2}\sum_{N=N_0}^{\infty} p_N\left|f_{DATI}^{(N)}(\mathbf{p}_N,\eta) + f_{RATI}^{(N)}(\mathbf{p}_N,\eta)\right|^2. \tag{27}$$

Analogously, the total ionization rate $\Gamma_{ion}(\eta)$ (or, in other words, the rate of total photoelectron and/or ion yields) due to photoionization of the initial atomic (ground) state can be found by means of integration of partial differential rates (26) over all angles of photoelectron emission and summation over all numbers N of incident photons absorbed:

$$\Gamma_{ion}(\eta) = \sum_{N=N_0}^{\infty}\int dO_{\mathbf{p}_N} w_{ATI}^{(N)}(\mathbf{p}_N,\eta) = \sum_{N=N_0}^{\infty} R_{ATI}^{(N)}(p_N,\eta). \tag{28}$$

IV. CALCULATIONS, NUMERICAL RESULTS, AND DISCUSSION

Thus, in the framework of the presently proposed strong-field ATI model, the high-energy photoelectron spectrum and respective PAD are represented by analytical expressions in closed and compact forms available for direct numerical calculations. According to Eqs. (13) and (22), these numerical calculations of ATI spectra are reduced first to accurate numerical calculation of generalized Bessel function $B_n(x;y)$ of integer order (corresponding to contributions of only open direct ATI channels) as well as subsequent taking a sufficient number of the most contributing ATI channels into proper account. The latter procedure is directly related to the way of effective numerical calculation of formally infinite sum in Eq. (22) over m corresponding to energy $\varepsilon_q^{(m)} = \mathbf{q}_m^2/2 = (m\omega - I_p - U_p)$ of an active (optical) electron in laser-field-induced resonance intermediate (essential) continuum states predominantly contributing to the amplitude of a certain photoelectron peak. This numerical procedure was already thoroughly justified earlier and verified under theoretical treatment of the HHG process in the framework of the currently applied strong-field approach (see also Ref. [36] for details). This procedure is reduced, in fact, to restriction of infinite number of terms in Eq. (22) by a finite number $m_{\max}$ corresponding to effective number $m_0 = m_{\max} - N_0$ of open ATI channels actually contributing to the total amplitude of the Nth photoelectron peak. Particularly, as was already ascer-

tained for partial amplitudes of the related HHG process, the number m_0 of predominantly contributing open ATI channels is always finite and proportional to a specified value of the Reiss parameter η only. To a fairly good accuracy, the number m_0 can be generally approximated by the value 4η, so that the further increase in the number of ATI channels taken into account ($m_{\max} \geqslant [N_0+4\eta]$) does not result in any essential changes in either the general shape of the produced high-energy ATI spectrum or the detailed structure of its conventional high-energy plateau. In this regard it is very interesting to note here that restricting the number m_0 by the value 2η (as suggested, in fact, by mentioned quasiclassical strong-field models) results in the arising of a secondary (but, quite a spurious) high-energy plateau in the after cutoff energy region ($\varepsilon_{\mathbf{p}} > \varepsilon_{cutoff} \approx 10U_p$) within which all photoelectron peaks are ascertained to exhibit a noticeably lower intensity (over about 6 to 7 orders of lesser magnitude) as compared to a conventional high-energy plateau region. Upon further increasing the number of ATI channels (e.g., $m_0=[3\eta]$, $[4\eta]$, etc.) taken into account under numerical calculations, the secondary plateau becomes highly suppressed, so that it is almost completely vanishing for $m_0 \geqslant [4\eta]$ owing to a considerable destructive interference. Thus, as was under consideration of the HHG process [36] within the framework of the same strong-field approach, the sufficient number of contributing open ATI channels taken into account should be also *at least twice more* than $m_0^{(class)}=[2\eta]$. The latter value is, in fact, the maximum possible number of open ATI channels taken into consideration by any semiclassical (simple-man-based) or quasiclassical strong-field ATI models due to the corresponding maximal value $q_{\max}=2(E/\omega)$ of intermediate canonical momentum suggested by the associated saddle-point method according to which *the classical return* back to the site of release is already impossible for photoelectrons released with canonical momentum larger than $2(E/\omega)$ [51] (see also the related discussion in Ref. [36]).

At last, according to the currently developed strong-field ATI model, all the information about the specified laser-irradiated system under consideration is obtained only via the ionization potential I_p, the Fourier transform $\Phi_0(\mathbf{q}) = \langle q|\Phi_0(\mathbf{r})\rangle$ of stationary wave function of initial discrete state $\Phi_0(\mathbf{r})$ and the Fourier transform $V(\mathbf{p}-\mathbf{q}) = \langle \mathbf{p}|\hat{V}(\mathbf{r})|\mathbf{q}\rangle$ of atomic binding potential $\hat{V}(\mathbf{r})$. Within the approximate ZRP (or δ potential) model for atomic binding potential $V(r)$ and corresponding ground discrete S-state $\Phi_0(\mathbf{r})$ with respective ionization potential $I_p=\kappa^2/2$, the exact analytical expressions

$$\Phi_0(\mathbf{q}) = \frac{\sqrt{\kappa}}{\pi}\frac{1}{(q^2+\kappa^2)}, \quad \langle \mathbf{p}|\hat{V}(\mathbf{r})|\mathbf{q}\rangle = \frac{1}{(2\pi\kappa)^2} \tag{29}$$

can be derived for these above-mentioned matrix elements which, following Refs. [19,21], will be also used in our further model numerical calculations. The ZRP model is well known as quite a conventional approximation for binding potential in atomic negative ions [52] and the hydrogen negative ion H^-, in particular. However, the ZRP model seems to be still a reasonable approximation for qualitative description of strong-field multiphoton phenomena in neutral atomic and molecular species [18,19,21–24,32,47,48,51,53,54], so that, to a reasonably good accuracy, expressions (29) can be also used under model calculations of the photoelectron spectrum produced by laser-exposed species others than negative ions. As appropriate representative examples of such calculations within the currently proposed ATI model, the photoelectron spectra produced by the ZRP-bound ''hydrogen'' atom are presented in Fig. 1 for different angles θ of electron emission with respect to the direction of incident field polarization **e**. These spectra were all calculated according to Eq. (26) under conditions of previous calculations within a different (though, also based on the ZRP model for atomic binding potential) quantum-mechanical strong-field approach [24] as well as considered earlier in Ref. [17] within the framework of pure numerical (the so-called B-spline) TDSE approach. By direct comparison one can see that all the currently calculated ATI spectra demonstrate an excellent accordance with respective spectra (see Fig. 3 presented in Ref. [24] and relevant Fig. 2 in Ref. [17], for comparison) both in general shape (e.g., the extent of the high-energy plateau and the value of its cutoff energy) and even reproduce the detailed structure. Particularly, the presented photoelectron spectrum corresponding to the angle $\theta=0$ fairly well recovers the conventional semiclassical ''$\varepsilon_{cutoff} \approx 10U_p$'' rule for the extent of the high-energy plateau and position of its cutoff energy. In this regard, it is quite appropriate to note here that, according to the currently developed model (but, unlike the semiclassical simple-man-based interpretation), the high-energy plateau cutoff appears to be strongly related to the particular asymptotic property of generalized Bessel function (5) for

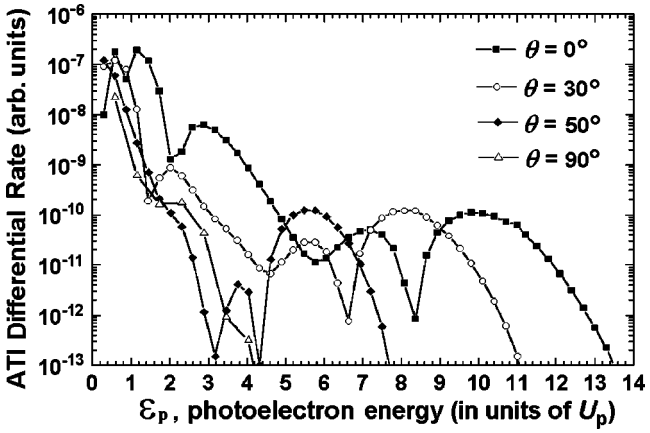

FIG. 1. Differential photoelectron spectra $w_{ATI}^{(N)}(\mathbf{p}_N, \eta)$ for ionization of a hydrogen atom by the laser radiation field of $\hbar\omega = 2$ eV, $I=2\times10^{14}$ W cm^{-2} corresponding to ponderomotive energy $U_p \approx 7.2$ eV, the Reiss parameter $\eta=3.58$, and the value of Keldysh parameter $\gamma=\omega\sqrt{2I_p}/E=0.986$. The spectra were calculated according to Eq. (26) for various angles θ of photoelectron emission with respect to the direction of incident field polarization: $\theta=0°$ (solid squares), $\theta=30°$ (open circles), $\theta=50°$ (solid diamonds), and $\theta=90°$ (open triangles). The electron energy is plotted in multiples of U_p; the symbols are joined by lines to guide the eye. This figure is to be compared with Fig. 3 presented in Ref. [24] and Fig. 2 in Ref. [17].

large values of the order n, namely, at fixed values of the arguments x and y, it is a very quickly decreasing function $[B_n(x;y)\rightarrow 0]$ of the order n beginning from $n \geqslant n_0 \sim |x| + 2|y|$ only. According to this alternative interpretation, the extent of the high-energy plateau is determined by values of the arguments $\zeta(\mathbf{p}) = (\mathbf{Ep})/\omega^2$ and $\eta = U_p/\omega$ of the generalized Bessel function (5) which, thus, restrict the effective (maximal) number n_0 of incident photons absorbed in the high-energy ATI process. For the same reason, the extent of the high-energy plateau is also strongly dependent on the angle θ due to the angle-dependent argument $\zeta(\mathbf{p}) = (\mathbf{Ep})/\omega^2 \sim \cos\theta$ of ordinary Bessel function $J_{m-N}(\zeta(\mathbf{p} - \mathbf{q}_m))$ contained in expression (22) derived for the rescattering ATI amplitude. Thus, Fig. 1 also clearly demonstrates the effect of considerable shrinking of the high-energy plateau (due to diminishing the value of its cutoff energy along with increasing the angle θ) that is in an excellent agreement with a general behavior of ATI spectra revealed in relevant experiments (e.g., in Ref. [7]) and results of earlier alternative theoretical calculations (e.g., Refs. [21–24,50]).

Figure 2(a) exhibits the results of calculation according to the currently proposed strong-field ATI model for ionization of an other ZRP-bound model atomic system (the so-called ''helium'' atom) under the conditions of high-energy ATI experiment [7] made with a neutral helium atom irradiated by the field of Ti:sapphire laser ($\omega = 1.6$ eV) corresponding to $U_p \approx 44.6$ eV, $\eta = 27.9$ and $\gamma = 0.525$ [see Fig. 2(b) in which the relevant experimental results are also presented for comparison]. A very extended plateau is the most prominent feature of ATI spectra presented for various values of angle θ of photoelectron emission with respect to the direction of incident field polarization, and for each angle the plateau has a very defined cutoff. Particularly, for emission of the photoelectron along the direction of incident field ($\theta = 0$), the calculated position of cutoff energy is a bit farther than $10U_p$, whereas the referred experimental results show the plateau cutoff at a noticeably smaller electron energy than the conventional semiclassical value $10U_p$. This deviation can be surely ascribed to a particular fact that in our calculations we had to use the value $I = 8 \times 10^{14}$ W cm^{-2} reported in Ref. [7] of laser intensity which was apparently just a peak value (e.g., in the very center of laser focus), whereas the actual (i.e., pulse- and focus-averaged) intensity attained in experiments [7] might be somewhat lower. For larger values of θ the high-energy plateau cutoff appears earlier than $10U_p$ (but, still noticeably farther than corresponding experimental results) that is, however, in a general accordance with calculations of completely classical [29] and quantum-mechanical strong-field ATI models (e.g., [21]). At the same time, in Fig. 2(a) there is a fairly good agreement with experimental results in respect of absolute peak heights (ionization rates) both in the low-energy region (where the direct ATI process is predominant) and in the high-energy plateau region (where the rescattering ATI process is predominant) as well as relative difference (of about five or six orders of magnitude, in average) in heights of photoelectron peaks between these energy regions. At last, even within the lower-energy region, the contribution of the direct ATI process always becomes smaller for larger values of θ, which is also generally consistent with relevant results of SFA-based quantum-mechanical calculations [21–24].

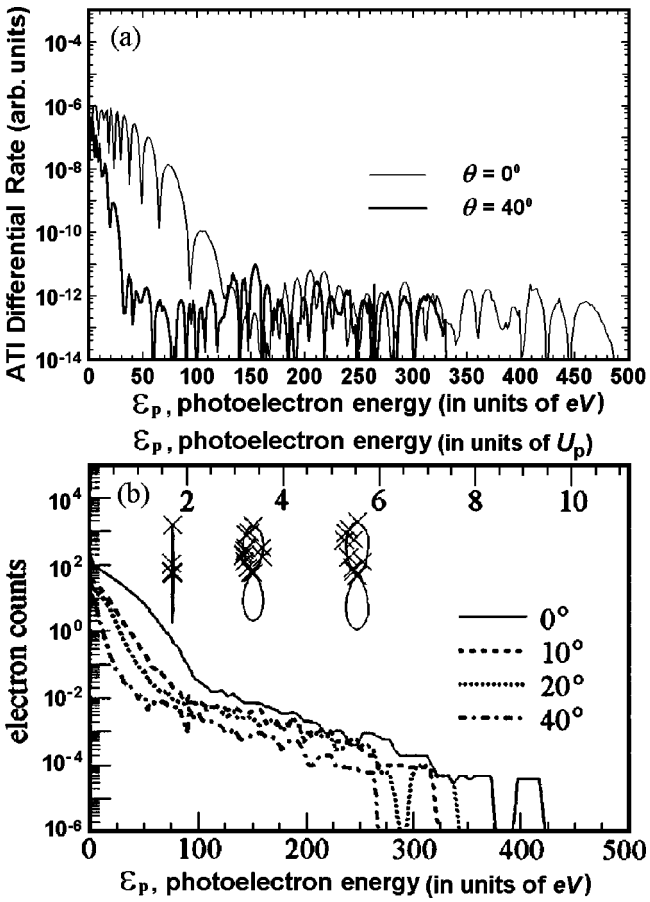

FIG. 2. Differential photoelectron spectra $w_{ATI}^{(N)}(\mathbf{p}_N, \eta)$ for ionization of a helium atom by the radiation field of Ti:sapphire laser ($\hbar\omega = 1.6$ eV, $I = 8 \times 10^{14}$ W cm^{-2}, corresponding to $U_p \approx 44.6$ eV, $\eta \approx 28$, and $\gamma = 0.525$), represented for various angles θ of photoelectron emission with respect to the direction of incident field polarization. (a) The spectra calculated according to the currently proposed strong-field ATI model: $\theta = 0°$ (thin line) and $\theta = 40°$ (thick line). (b) The spectra corresponding to relevant experimental data of Ref. [7] (see also Fig. 1 presented therein): $\theta = 0°$ (solid line), $\theta = 10°$ (dashed line), $\theta = 20°$ (dotted line), $\theta = 40°$ (dash-dotted line). The symbols are omitted, but joined by lines, so that only the envelopes of photoelectron peaks in each spectrum are presented. These photoelectron spectra are also very reminiscent of those calculated in Ref. [21] for a helium atom under comparable values of parameters of the incident laser field (see Fig. 1 therein).

Besides the dependence of a general form of high-energy photoelectron spectrum and its detailed structure on major parameters of the incident radiation field and specified laser-exposed system, it seems to be also very interesting to investigate separate contributions of the direct and rescattering ATI processes relative to each other and analyze their comparative roles in the formation of the produced photoelectron spectrum. Figures 3(a) and 3(b) demonstrate the photoelectron spectra calculated according to Eqs. (13), (22), and (26) for above-threshold photodetachment (ATD) of negative hydrogen ion H^- by linearly polarized CO_2-laser radiation under initial conditions considered in Ref. [50] within the

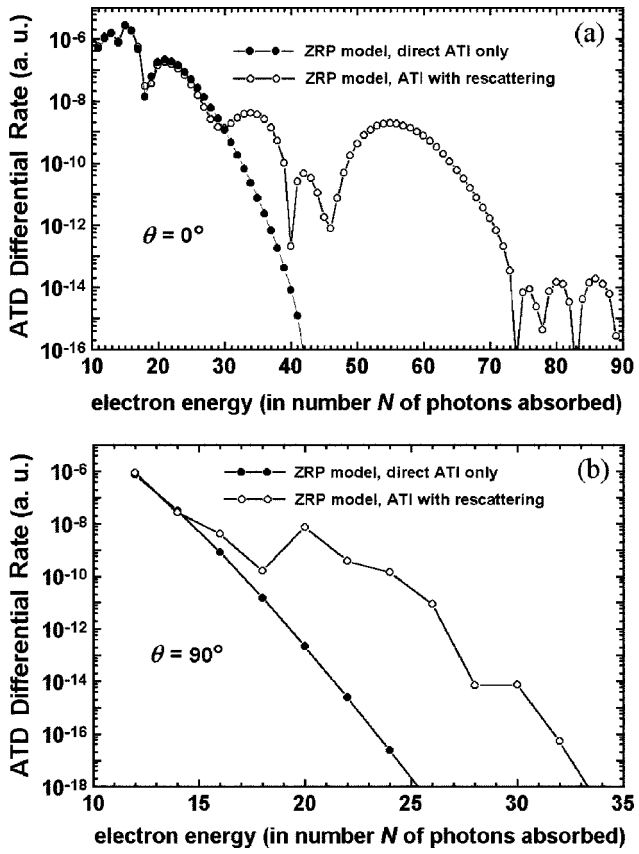

FIG. 3. Differential photoelectron spectra $w_{ATI}^{(N)}(\mathbf{p}_N,\eta)$ for a negative hydrogen ion H^- photodetachment by CO_2-laser radiation ($\hbar\omega=0.117$ eV, $I=5\times10^{10}$ W cm^{-2}, so that $U_p\approx0.52$ eV, $\eta=4.46$, and $\gamma=0.85$) calculated for various values of angle θ of photoelectron emission with respect to the direction of incident field polarization: (a) $\theta=0°$; (b) $\theta=90°$. Solid circles correspond to photoelectrons produced due to direct ATD process only, whereas open circles correspond to photoelectrons produced due to the direct and rescattering ATD processes taken into account. The energy of photoelectron peaks is plotted in units of total number N of absorbed photons; the symbols are joined by lines to guide the eye. These figures are to be compared with Fig. 5 presented in Ref. [50].

framework of a modified SFA-based quasiclassical approach (the so-called atomic antenna mechanism, see, e.g., the relevant results presented in Fig. 5 therein) and corresponding to $U_p\approx0.52$ eV, $\eta=4.46$, and $\gamma=0.85$. All spectra presented in Figures 3(a)–3(b) were calculated for two values of the angle θ (0 and $\pi/2$) of photoelectron emission with respect to the direction of incident field polarization and these spectra are in an excellent agreement with respective results of Ref. [50], in both a general form and even detailed structure. In particular, for emission of a photoelectron along the direction of incident field polarization ($\theta=0$), the position of calculated cutoff energy $\varepsilon_{cutoff}=\varepsilon_{\mathbf{p}}^{(N_{cutoff})}\approx10U_p=(N_{cutoff}-N_0)\omega\approx45\omega$ exactly corresponds to the total maximal number $N_{\max}\approx56$ of photons absorbed and minimal possible number $N_0=[(I_p+U_p)/\omega]+1\approx11$ of absorbed photons required for ionization. In addition, the results corresponding to the contribution of the standard Keldysh amplitude (13), taking into account only the direct ATI process, are also given separately in the same figures and well seen to be predominant mostly within the low-energy part of the photoelectron spectrum only. So, for emission of photoelectrons along the direction of incident field ($\theta=0$) this contribution is almost precisely coincident with the total photoelectron spectrum within the relatively low-energy region $0\leqslant\varepsilon_{\mathbf{p}}\leqslant2U_p\approx(30-N_0)\omega$ where the rescattering process contributes negligibly. However, beyond this region (i.e., within the high-energy plateau region $2U_p\leqslant\varepsilon_p\leqslant10U_p$) the photoelectron spectrum consists almost entirely of the contribution from rescattered electrons. For the particular case of incident laser field of linear polarization and spherically symmetric atomic binding potential under consideration, it is also very interesting to note here that only even total net numbers N of photons are absorbed by the photoelectrons emitted at the angle $\theta=0$. The latter means that only photoelectron peaks corresponding to even number $N=(\mathbf{p}_N^2/2\omega+I_p+U_p)/\omega$ of absorbed photons (and, thus, separated from each other by double fundamental frequency) can be observed along the direction that is perpendicular to the incident laser field polarization [Fig. 3(b), see also Fig. 1 and the line corresponding to $\theta=90°$ therein]. The latter feature noted at $\theta=90°$ is quite a natural and direct consequence of dipole (or *long-wavelength*) approximation due to neglecting any photon momenta, $\mathbf{k}=0$. Particularly, within the framework of the currently applied strong-field approach, there is a very simple explanation for this noted feature, namely, it follows directly from the equation $\zeta(\mathbf{p}_N)=(\mathbf{E}\mathbf{p}_N)/\omega^2=0$ [i.e., in Eq. (22) we have, in fact, $J_{m-N}(\zeta(\mathbf{p}_N-\mathbf{q}_m))=J_{m-N}(\zeta(\mathbf{q}_m))$] as well as from the parity properties of Bessel functions contained in ATI amplitudes (13) and (22). Recall that $J_s(-x)=(-1)^sJ_s(x)$ and, accordingly, $B_s(-x;y)=(-1)^sB_s(x;y)$, so that the integrand function in Eq. (22) is always an even function of intermediate canonical momentum $\mathbf{q}$ under the replacement $\mathbf{q}\rightarrow-\mathbf{q}$. Consequently, the integral expression (22) for the amplitude of the rescattering ATI process of electron emission at the angle $\theta=90°$ is nonzero *only if* N is an even number. Analogously, from Eq. (13) it directly follows that the amplitude of the direct ATI process of electron emission at the angle $\theta=90°$ is nonzero *only for even* N only for which $B_{-N}(\zeta(\mathbf{p}_N);\eta/2)=B_{-N}(0;\eta/2)=J_{-N/2}(\eta/2)\neq0$; otherwise, for odd N, it immediately follows that $B_{-N}(0;\eta/2)\equiv0$ (see also, e.g., Ref. [37]).

The relative contributions of direct and rescattering ATI processes are also clearly seen to be even more distinct and distinguishable in respective integral photoelectron spectra calculated for ATD of negative hydrogen ion H^- irradiated by CO_2-laser and represented in Fig. 4 by integral photodetachment rates $R_{ATI}^{(N)}(p_N)$ (i.e., integrated over all angles of photoelectron emission) for different values of incident laser intensity. As compared to differential photoelectron spectra presented in Figs. 3(a) and 3(b), no randomly oscillating values are seen in Fig. 4 of photodetachment rates in calculated integral photoelectron spectra which are considerably more smooth and, within high-energy region, slowly varying with increasing of photoelectron energy (or the total number N of incident photons absorbed). Within the low-energy region all the calculated photoelectron spectra are in almost precise

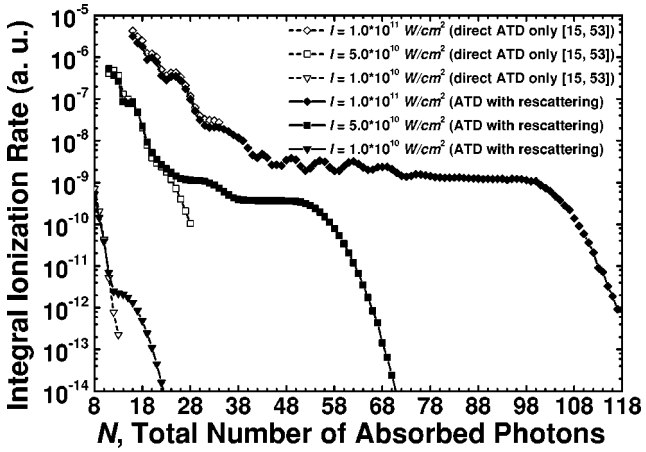

FIG. 4. Integral photoelectron spectra $R_{ATI}^{(N)}(p_N,\eta)$ for above-threshold photodetachment (ATD) of the negative hydrogen ion H^- by a radiation of the CO_2 laser ($\hbar\omega=0.117$ eV) calculated for various values of incident laser intensity: $I=1\times10^{10}$ W cm^{-2} (down triangles), $I=5\times10^{10}$ W cm^{-2} (squares), and $I=1\times10^{11}$ W cm^{-2} (diamonds). Open symbols correspond to earlier results of other authors for photoelectrons produced due to the direct ATD process only (see Table II presented in Ref. [15] and Table I presented in Ref. [53]), whereas solid symbols correspond to photoelectrons produced due to the ATD process with rescattering taken into account under calculations according to the current strong-field ATI model. The energy of photoelectron peaks is plotted in units of the total number N of absorbed photons; the symbols are joined by lines to guide the eye.

agreement with respective ones calculated by other authors under the same conditions, but within different strong-field photodetachment models [15,53] ignoring any rescattering ATD process. Some deviations are obviously caused by some minor contribution of the rescattering ATD process to the low-energy part of the spectrum taken into consideration under current calculations, but neglected in above-mentioned previous strong-field ATD models. Finally, as expected, the presently calculated photoelectron spectra also well demonstrate a rise of extension (the length) of the rescattering plateau (in an excellent accordance with the conventional phenomenological $10U_p$ rule) as well as its average level (or average height of high-energy photoelectron peaks within the rescattering plateau region) with increasing the incident laser intensity: namely, according to the mentioned semiclassical rule one should expect that the number of absorbed photons corresponding to the high-energy plateau cutoff are to be $N_{cutoff}=17$ for laser intensity $I=1\times10^{10}$ W cm^{-2}, whereas $N_{cutoff}=56$ for $I=5\times10^{10}$ W cm^{-2} and $N_{cutoff}=106$ for $I=1\times10^{11}$ W cm^{-2}.

The numerical results for anomalous PAD calculated according to the proposed strong-field ATI model and corresponding to a separate high-energy photoelectron peak within the rescattering plateau region are represented in Figs. 5(a)–5(d) for the ATD process of negative hydrogen ion H^- under the conditions used in our previous calculations of respective photoelectron spectra presented in Fig. 3 above. All the presently calculated PAD are well seen to be in a fairly good accordance with the relevant results of earlier alternative calculations for respective PAD within a different strong-field (viz., the atomic antenna) approach [50] (see the relevant Fig. 3 presented therein). Due to linear polarization of incident laser field and implicit assumption about central (spherical) symmetry of the atomic binding potential under consideration, those angular distributions are expected to have an azimuthal symmetry with respect to the field polarization axis, therefore only the dependence on the polar

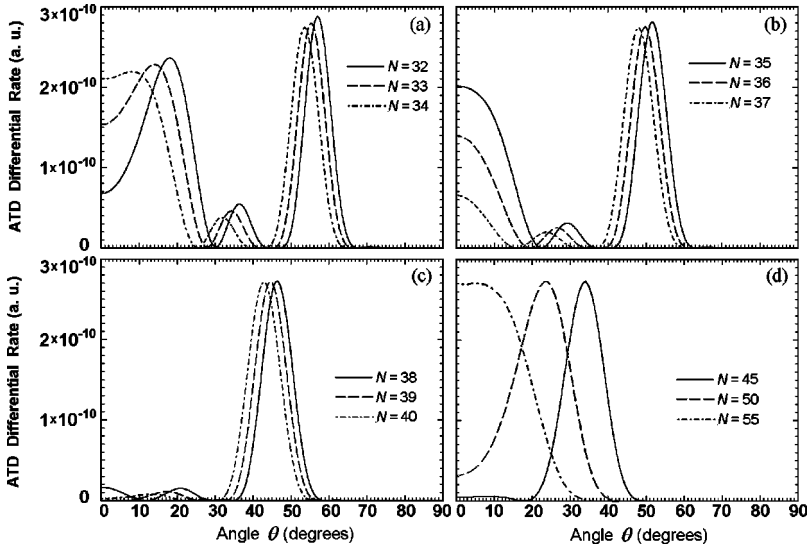

FIG. 5. Partial photoelectron angular distributions $w_{ATI}^{(N)}(\mathbf{p}_N,\eta)$ corresponding to various photoelectron peaks in the spectrum of negative hydrogen ion H^- photodetachment by CO_2-laser radiation ($\hbar\omega=0.117$ eV, $I=5\times10^{10}$ W cm^{-2}, so that $U_p\approx0.52$ eV, $\eta=4.46$, and $\gamma=0.85$), all calculated according to formula (28) and represented as functions of the angle θ of electron emission with respect to the direction of incident field polarization. The energy of the photoelectron peak is presented in units of the total number N of absorbed photons: (a) $N=32$ (solid line), $N=33$ (dashed line), $N=34$ (dash-dotted line); (b) $N=35$ (solid line), $N=36$ (dashed line), $N=37$ (dash-dotted line); (c) $N=38$ (solid line), $N=39$ (dashed line), $N=40$ (dash-dotted line); (d) $N=45$ (solid line), $N=50$ (dashed line), $N=55$ (dash-dotted line). These figures are to be compared with Fig. 5 presented in Ref. [50].

angle θ between the directions of photoelectron emission and incident field polarization is depicted in Figs. 5(a)–5(d). As is well known, the angular distributions of direct photoelectrons (i.e., primarily corresponding to low-energy photoelectron peaks within the region $0 \leqslant \varepsilon_p \leqslant 2U_p$) are generally strongly aligned along the incident field polarization direction and become narrower toward the limit $2U_p$ [8]. However, essential and drastic changes are present in angular distributions of rescattered photoelectrons with energies higher than $2U_p$, namely, within the rescattering plateau region of energy the respective PAD become noticeably broader, though are gradually narrowing on further increasing the electron energy towards the value $10U_p$ corresponding to the plateau cutoff. Thus, Figs. 5(a)–5(d) also confirm and well illustrate this general rule, moreover, it is also well seen that a noticeably larger part of photoelectrons of energy higher than $2U_p$ is emitted along spatial directions different from the incident field polarization, so that the corresponding PAD are getting concentrated mainly in a few separate narrow regions (the so-called side-lobes or rings) which are centered at values of the angle θ different from zero. Whereas, for photoelectrons of energy nearer to the plateau cutoff region $\varepsilon_p \approx 10U_p$ [the line corresponding to $N=55$ in Fig. 5(d)] the ringlike structure in PAD gradually disappears, and, simultaneously, the total width of respective PAD becomes noticeably narrower, being centered at the direction of incident field polarization (see also Ref. [18]).

At last, it seems to be also interesting to apply the proposed ATI model to laser-exposed atomic species bound to a different, more realistic binding potential $V(\mathbf{r})$, instead of the previously used ZRP model, and compare the respective resulting photoelectron spectra. As was suggested in Ref. [22], let us also consider, for example, a laser-irradiated ''He'' atom bound with short-range Yukawa model potential $\hat{V}(\mathbf{r}) = -Zr^{-1}\exp(-\lambda r)$ (or, the so-called ''screened'' Coulomb potential). However, unlike Ref. [22] [where $Z=1$ and $\kappa = \sqrt{2I_p}=1$ were implied, i.e., the exact $1S$-state wave function of a hydrogen atom was used, in fact, as initial ground discrete state of the He atom for calculation of relevant matrix element $\Phi_0(\mathbf{p})$], it seems to be more natural to suppose $Z=2$ for a neutral He atom under our numerical calculations. The latter supposition can also provide the exact value of initial ground-state energy $\varepsilon_0 = -I_p = -0.9036$, whereas the reasonable value of κ corresponding to this correct binding energy of the initial ground state can be found, for example, by means of the following trial variational wave function:

$$\Phi_0(\mathbf{r}) = \frac{\kappa^{3/2}\exp(-\kappa r)}{\sqrt{\pi}}. \tag{30}$$

Here κ is some variational parameter introduced to minimize the ground-state energy $\varepsilon_0(\lambda)$ of such a neutral He atom bound with Yukawa potential and, simultaneously, to provide the correct value of $\varepsilon_0(\lambda) = -0.9036$. One can derive that, in order to comply with these two conditions, parameters λ and κ (related to each other by the relation $p = 2\kappa\lambda^{-1} > 1$) should satisfy the following equations (see, e.g., Ref. [55]):

$$\frac{2p^4(p-1)(p+3)}{(p+1)^6} = 0.9036, \quad \lambda^{-1} = \frac{(p+1)^3}{4p(p+3)}. \tag{31}$$

There is only one, a single, real positive root $p \approx 5.32$ that can be immediately found out from these two equations, so that $\lambda \approx 0.701$ and, hence, $\kappa \approx 1.866$. Finally, the respective expressions for the matrix elements $\Phi_0(\mathbf{q})$ and $V(\mathbf{p}-\mathbf{q})$ in final analytical expressions (13) and (22) corresponding to the short-range Yukawa model binding potential take the form

$$\Phi_0(\mathbf{q}) = \frac{2\sqrt{2}\kappa^{5/2}}{\pi(\mathbf{q}^2+\kappa^2)^2}, \quad \langle \mathbf{p}|\hat{V}(\mathbf{r})|\mathbf{q}\rangle = -\frac{1}{\pi^2}\frac{1}{(\mathbf{p}-\mathbf{q})^2+\lambda^2}. \tag{32}$$

The resulting photoelectron spectra for ionization of such a neutral He atom by the field of yttrium aluminum garnet (YAG) laser are presented in Figs. 6(a) and 6(b). These spectra were calculated according to Eq. (26) under conditions considered in Ref. [22] for two different models of atomic binding potential—either the Yukawa model potential (though, with the corrected values of parameters λ and κ found above) or the ZRP model [with corresponding expressions (29) for the respective matrix elements $\Phi_0(\mathbf{q})$ and $V(\mathbf{p}-\mathbf{q})$ and parameter $\kappa = 1.345$ corresponding to the binding energy $\varepsilon_0 = -\kappa^2/2 \approx -24.6$ eV used for the neutral ZRP He atom]. As expected, there is a noticeable difference seen in calculated photoelectron spectra produced by the model Yukawa He atom relative to the ZRP He atom and, particularly, a difference in the average level of heights (intensities) between low-energy and high-energy photoelectron peaks: namely, the relative difference in the average level of heights of low-energy and high-energy photoelectron peaks has been found to be about 5–6 orders of magnitude in the calculated spectrum corresponding to the Yukawa He atom (with $\lambda \approx 0.701$), i.e., it is slightly increased as compared to about 4–5 orders of magnitude for the respective difference found in the photoelectron spectrum calculated for the model ZRP He atom. This particular feature is also well seen in the lower-energy part of the same spectra presented separately in Fig. 6(b); thus, the results of our present calculations generally confirm the effect of dependence of the relative difference in heights of low-energy and high-energy photoelectron peaks (found in Ref. [22] for a model laser-irradiated Yukawa He atom) on a specified value of the screening parameter λ. However, according to our present calculations (but, contrary to alternative recent results of Ref. [22]), this dependence proved to be inessential, so that the related change of the relative difference is not too large (viz., nearly about one order of magnitude in average), versus a very huge relative difference (of about 12–14 orders of magnitude) revealed in the photoelectron spectra calculated in Ref. [22] for a Yukawa He atom with similarly small screening parameters λ. In this regard, it is worth reminding that, under numerical calculations of photoelectron spectra corresponding to different values of λ used in Ref. [22] for a Yukawa He atom, the value of binding energy ($\varepsilon_0 = -0.5$) would be rather appropriate for the hydrogen atom only. Moreover, the value ε_0

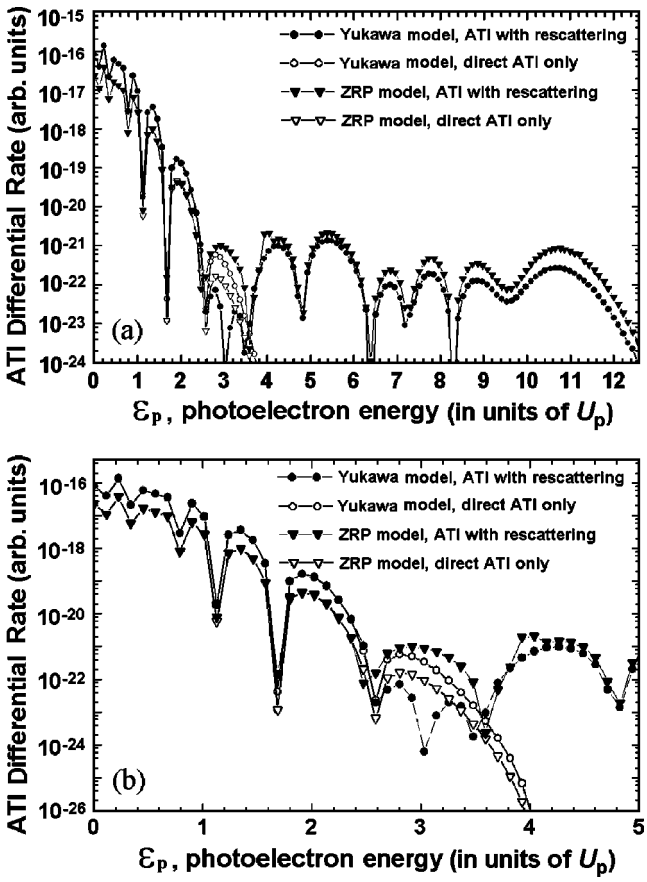

FIG. 6. (a) Differential photoelectron spectra $w_{ATI}^{(N)}(\mathbf{p}_N,\eta)$ for ionization of the neutral He atom by the radiation field of the YAG laser ($\hbar\omega=1.17$ eV, $I=1\times10^{14}$ W cm^{-2} corresponding to $U_p\approx10.43$ eV, $\eta\approx8.9$, and $\gamma\approx1.086$) and calculated for photoelectron emission along the polarization of incident laser field ($\theta=0°$). The presented spectra were calculated for two different models of the atomic binding potential: either the model Yukawa (screened Coulomb) potential with variational value of screening parameter $\lambda\approx0.701$ (circles) or the ZRP model (down triangles). (b) The low-energy part of the spectra presented in (a) also showing clearly the respective separate contribution of the direct ATI process only (the open symbols) vs the total spectra with the rescattering ATI process taken into account (the solid symbols). The electron energy is plotted in multiples of U_p; the symbols are joined by lines to guide the eye. These figures are to be compared with Fig. 1(a) presented in Ref. [22].

was supposed to be quite independent on the screening parameter λ that also seems to be physically incorrect. The latter means, particularly, that the mentioned strikingly fast (both absolute and relative) rise of the total probability rates in the low-energy region of photoelectron spectra calculated in Ref. [22] for similar values of parameter λ of the Yukawa He atom cannot be explained and sufficiently well justified by just a different form of atomic binding potential only (as suggested, in fact, in Ref. [22]). Therefore, the associated main conclusion of Ref. [22] predicting a principal possibility of effective control of the height of the rescattering plateau by just changing the screening parameter λ seems to be at least quite questionable. The latter noted particular contradiction is mainly caused by the relative contribution of the direct ATI process that was enormously overestimated in Ref. [22] *due to a different representation* (viz., via the matrix element $V_0(\mathbf{p})=\langle\mathbf{p}|\hat{V}(\mathbf{r})|\Phi_0(\mathbf{r})\rangle$ of interaction with an atomic binding potential) utilized to derive the respective Keldysh amplitude which is always predominant within the low-energy region only. Recall, however, that the latter mentioned representation used in Ref. [22] *is physically equivalent* to the currently used one [i.e., via matrix element of em interaction $\hat{W}(\mathbf{r},t)$, which is some kind of standard for the direct ATI amplitude in all KFR theories [42]] *only provided the exact wave functions* of the considered laser-irradiated atomic system *are used* under final numerical calculations. Meanwhile, within the Yukawa model for atomic binding potential, one has to use only approximate wave functions and this latter approximation may inevitably cause a great difference in final results of calculations. This latter conclusion becomes also especially evident from the later results of Ref. [23] calculated by the same authors within a newer (improved) version of their quasiclassical ATI model where the conventional representation [i.e., via matrix element of em interaction $\hat{W}(\mathbf{r},t)$ with an incident laser field] was used and, additionally, the Coulomb effects were also taken into some account. Although the Coulomb effects were identified there as responsible for a considerable increase of the ionization rates that should change the behavior of the rates in the lower-energy region, nevertheless, there was no any enormously increased huge relative difference yet found in Ref. [23] for average level of heights of lowest photoelectron peaks with respect to high-energy ones previously calculated and reported about in Ref. [22] for small screening parameter λ. This conclusion is also generally consistent with the spectrum presented in Figs. 6(a) and 6(b) for the Yukawa He atom and calculated for the correct value of its binding energy and more realistic value $\lambda\approx0.701$ of the screening parameter, so that the respective spectrum demonstrates a behavior very similar to the results corresponding to the model ZRP He atom for which the matrix elements (29) are exact due to the fact that the ZRP model allows to have deal only with exact solutions for wave functions used under calculations. Thus, the ZRP model, essentially exploited in our current calculations only for correct comparison with relevant results of different approaches, again proved to be still quite a reasonable approximation for model (simplified) numerical calculations of strong-field phenomena in atomic systems. Particularly, this approximation is still available for adequate qualitative (and, to a reasonable accuracy, even quantitative) description of photoelectron spectra produced due to the high-energy ATI process in various atomic species including negative ions.

V. CONCLUSION

Thus, the highly nonlinear multiphoton strong-field process of high-energy above-threshold ionization in an isolated atomic system irradiated by an intense laser radiation was considered theoretically and studied numerically within the framework of an alternative nonrelativistic fully quantum-mechanical strong-field approach that we developed earlier for theoretical treatment of high-order harmonic generation.

The underlying approach is based on the standard *Keldysh approximation* combined with the essential states method (and the associated *pole approximation*), which, applied together, allow for representation of the total ATI amplitude in a closed and compact (the so-called *factorized*) analytical form. The related proposed strong-field ATI model also describes a highly nonperturbative (though, also single-active-electron) response to incident laser field in terms of a superposition of two nonlinear processes—*the direct ATI process* of emission of relatively low-energy photoelectrons (with energies extending up to about $2U_p$) and *the rescattering ATI process* of high-energy electrons emission (of energies extending up to $10U_p$). The applied strong-field approach is fully quantum mechanical and developed beyond any semiclassical concepts of the most contributing classical trajectories (or *quantum paths*) of the released electron being in intermediate continuum states. Therefore, the developed ATI model does not require any numerical analysis of the released electron classical motion along complex trajectories for finding out and consequent thorough selection of only those which contribute predominantly to the amplitude of the photoprocess under consideration. This, particularly, means that all the mentioned contributing classical trajectories are *ab initio* taken into proper consideration (irrespective of the initial value of the released electron velocity v_0) provided the number of contributing open ATI channels taken into account under numerical calculations is sufficiently large to suppress the secondary (though, quite a spurious) high-energy ATI plateau. In addition, the proposed ATI model is not restricted to one-dimensional consideration only corresponding to motion of the released electron ejected to intermediate continuum states either along the polarization of incident laser field or opposite one. Indeed, this model always and *automatically* takes also those trajectories of released electrons that are ejected under an arbitrary angle in respect of the incident field polarization into equal account; this latter procedure is just reduced to performing of internal numerical integration in Eq. (24) over all intermediate angles of released electron ejection.

Application of the *pole approximation* proved to be extremely useful and working surprisingly well, it also makes the final results quite transparent for interpretation (particularly, the direct ATI process and rescattering ATI process are found to be strongly interrelated) and allows for deriving the final expressions for ATI probability rates in a closed analytical form available for direct numerical calculations. On the other hand, this considerably simplifies the problem as it also allows one to take into proper consideration both arbitrary incident laser fields (of various frequencies and polarization compositions and spatial configurations) and arbitrary binding potentials (insomuch, as their Fourier transforms can be obtained in a closed analytical form). Although the saddle-point approximation can do the latter (i.e., to treat arbitrary binding potentials) too, but not for the exact solution of the strong-field approximation, which is, thus, always restricted to a model zero-range potential only that seems to be quite inconvenient for extension to other laser-irradiated systems (e.g., molecule, etc.) more complex than atomic one. It should be also mentioned that, as in Ref. [37] (but unlike the most of other authors) the "*velocity*" gauge of em interaction (1) with incident laser field is substantially used in the currently proposed strong-field ATI model, otherwise the model would be much more cumbersome in the more commonly used "*length*" gauge.

To verify and demonstrate a remarkably good applicability (and availability) of the proposed model, a number of photoelectron spectra produced by various specified atomic species (mostly noble gas atoms and negative ions) and associated photoelectron angular distributions (the so-called sidelobes or rings) have been calculated and shown to fairly well reproduce the conventional semiclassical "$\varepsilon_{cutoff} \approx 10U_p$" rule for the extent of the high-energy plateau and the position of its cutoff energy. The results of our numerical calculations unambiguously proved that the currently proposed strong-field ATI model is equally well applicable and available for effective numerical calculation of atomic photoelectron spectra, especially, having a very long high-energy plateau. The model also describes adequately (the better, the larger the value of the Reiss parameter η is) both the general shape and detailed structure of high-energy photoelectron spectra as well as their nonlinear behavior within a broad and the most interesting region of the problem parameters. All the representative photoelectron spectra currently calculated as illustrative examples are also in an excellent or fairly good accordance with those observed in relevant experiments and/or calculated within quite different (though, often either too analytically cumbersome or very demanding computationally) approaches and methods developed earlier by other authors. Finally, due to the fact that the related numerical calculations are considerably more facilitated compared to previously developed different strong-field models, the advantages of the currently proposed strong-field ATI model make it especially promising and helpful for theoretical treatment of the high-energy ATI process, e.g., in much more complex laser-irradiated species (molecules, etc.) or in the particular case of two-color (bichromatic) incident laser field of nonstandard frequency and polarization composition and arbitrary spatial configuration, which are very important for various fascinating practical applications.

ACKNOWLEDGMENTS

The authors are indebted and very grateful to Dr. Wilhelm Becker and Professor Valentin N. Ostrovsky for their valuable remarks and helpful and stimulating discussions during the preparation of this paper. One of us (V.I.U.) also gratefully acknowledges the support from DAAD (Deutscher Akademischer Austauschdienst) and would like to express his gratitude for the hospitality and additional support kindly extended to him by Dr. Wolfgang Sandner and Dr. Wilhelm Becker as well as thank Dr. R. Kopold from B-Division of the Max-Born-Institute of Nonlinear Optics and Short-Pulse Spectroscopy (Berlin) for permanent everyday help during his working visit. The research described in this publication was also made possible in part by financial support (Award No. ZP2-2279) by the U.S. Civilian Research and Development Foundation (CRDF) for the Independent States of the Former Soviet Union.

[1] J.H. Eberly, J. Javanainen, and K. Rzazewski, Phys. Rep. **204**, 331 (1991).
[2] *Multiphoton Processes*, Proceedings of the ICOMP-99 Conference, edited by L.F. DiMauro, R.R. Freeman, and K.C. Kulander, AIP Conf. Proc. No. 525 (AIP, Melville, NY, 2000).
[3] Y. Gontier, M. Poirier, and M. Trahin, J. Phys. B **13**, 1381 (1980).
[4] P. Agostini *et al.*, Phys. Rev. Lett. **42**, 1127 (1979).
[5] G. Manfray and C. Manus, Rep. Prog. Phys. **54**, 1333 (1991).
[6] G.G. Paulus *et al.*, Phys. Rev. Lett. **72**, 2851 (1994).
[7] B. Walker *et al.*, Phys. Rev. Lett. **77**, 5031 (1996).
[8] B. Yang *et al.*, Phys. Rev. Lett. **71**, 3770 (1993).
[9] L.F. DiMauro and P. Agostini, Adv. At., Mol., Opt. Phys. **35**, 79 (1995).
[10] M. Protopapas, C.H. Keitel, and P.L. Knight, Rep. Prog. Phys. **60**, 389 (1997).
[11] C.J. Joachain, M. Dörr, and N. Kylstra, Adv. At., Mol., Opt. Phys. **42**, 225 (2000).
[12] J.H. Eberly, Q. Su, and J. Javanainen, Phys. Rev. Lett. **62**, 881 (1989).
[13] E. Huens, B. Piraux, A. Bugacov, and M. Gajda, Phys. Rev. A **55**, 2132 (1997).
[14] X.M. Tong and Shih-I Chu, Int. J. Quantum Chem. **69**, 293 (1998); Phys. Rev. A **57**, 452 (1998).
[15] D.A. Telnov and S.I. Chu, Phys. Rev. A **50**, 4099 (1994); J. Phys. B **29**, 4401 (1996).
[16] J. Zakrzevsky and D. Delande, J. Phys. B **28**, L667 (1995).
[17] E. Cormier and P. Lambropoulos, J. Phys. B **30**, 77 (1997).
[18] W. Becker, A. Lohr, and M. Kleber, J. Phys. B **27**, L325 (1994).
[19] W. Becker, A. Lohr, and M. Kleber, Quantum Semiclass. Opt. **7**, 423 (1995).
[20] M. Lewenstein *et al.*, Phys. Rev. A **51**, 1495 (1995).
[21] A. Lohr, M. Kleber, R. Kopold, and W. Becker, Phys. Rev. A **55**, R4003 (1997).
[22] D.B. Milosevic and F. Ehlotzky, Phys. Rev. A **57**, 5002 (1998).
[23] D.B. Milosevic and F. Ehlotzky, Phys. Rev. A **58**, 3124 (1998).
[24] R. Kopold and W. Becker, J. Phys. B **32**, L419 (1999).
[25] R. Kopold, D.B. Milosevic, and W. Becker, Phys. Rev. Lett. **84**, 3831 (2000).
[26] R. Kopold, W. Becker, and M. Kleber, Opt. Commun. **179**, 39 (2000).
[27] P.B. Corkum, N.H. Burnett and F. Brunel, in *Atoms in Intense Fields*, edited by M. Gavrila (Academic, Boston, 1992), p. 109.
[28] P.B. Corkum, Phys. Rev. Lett. **71**, 1994 (1993).
[29] G.G. Paulus *et al.*, J. Phys. B **27**, L703 (1994).
[30] M.B. Smirnov and V.P. Krainov, J. Phys. B **31**, L519 (1998).
[31] G.G. Paulus, W. Becker, and H. Walther, Phys. Rev. A **52**, 4043 (1995).
[32] C.F. de Morisson Faria *et al.*, Phys. Rev. A **60**, 1377 (1999).
[33] D.B. Milosevic and B. Piraux, Phys. Rev. A **54**, 1522 (1996).
[34] D.B. Milosevic, W. Becker, and R. Kopold, Phys. Rev. A **61**, 063403 (2000).
[35] S. Long, W. Becker, and J.K. McIver, Phys. Rev. A **52**, 2262 (1995).
[36] V.I. Usachenko and V.A. Pazdzersky, J. Phys. B **35**, 761 (2002).
[37] H.R. Reiss, Phys. Rev. A **22**, 1786 (1980).
[38] Z. Deng and J.H. Eberly, J. Opt. Soc. Am. B **2**, 486 (1985).
[39] M.V. Fedorov, *Atomic and Free Electrons in a Strong Light Field* (World Scientific, Singapore, 1997).
[40] F. Ehlotzky, Phys. Rep. **345**, 175 (2001).
[41] N.B. Delone and V.P. Krainov, *Atoms in Strong Light Fields*, Springer Series Chemical Physics Vol. 28 (Springer-Verlag, Berlin, 1985).
[42] H.R. Reiss, Phys. Rev. A **42**, 1476 (1990); Prog. Quantum Electron. **16**, 1 (1992).
[43] L.V. Keldysh, Zh. Exp. Teor. Fiz. **47**, 1945 (1964) [Sov. Phys. JETP **20**, 1307 (1965)].
[44] M.P. Hertlein, P.H. Bucksbaum, and H.G. Muller, J. Phys. B **30**, L197 (1997); P. Hansch, M.A. Walker, and L.D. Van-Woerkom, Phys. Rev. A **55**, R2535 (1997).
[45] H.G. Muller, Phys. Rev. Lett. **83**, 3158 (1999); H.G. Muller and F.C. Kooiman, *ibid.* **81**, 1207 (1998).
[46] S.V. Popruzhenko, Ph.A. Korneev, S.P. Goreslavski, and W. Becker, Phys. Rev. Lett. **89**, 023001 (2002); R. Kopol'd, W. Becker, M. Kleber, and G.G. Paulus, J. Phys. B **35**, 217 (2002); B. Borca, M.V. Frolov, N.L. Manakov, and A.F. Starace, Phys. Rev. Lett. **88**, 193001 (2002).
[47] G.G. Paulus, F. Grasbon, H. Walther, R. Kopol'd, and W. Becker, Laser Phys. **12**, 262 (2002).
[48] M.Yu. Kuchiev, J. Phys. B **28**, 5093 (1995).
[49] M.Yu. Kuchiev and V.N. Ostrovsky, J. Phys. B **32**, L189 (1999); Phys. Rev. A **60**, 3111 (1999).
[50] M. Yu. Kuchiev and V.N. Ostrovsky, in *Atoms, Molecules and Quantum Dots in Laser Fields: Fundamental Processes, Pisa, 2000*, edited by N. Bloembergen, N. Rahman, and A. Rizzo (Societe Italiana di Fisica, Bologna, 2001), Vol. 71, p. 285; see also e-print physics/0010019v1.
[51] V.I. Usachenko and R.M. Galimzyanov, in Book of Abstracts of XV International Conference on Laser Spectroscopy ICOLS-2001 (Snowbird, Utah, 2001) (unpublished), Abstract pp. 2–32.
[52] Yu. N. Demkov and V.N. Ostrovsky, *Zero-Range Potential and Its Application in Atomic Physics* (Plenum, New York, 1988).
[53] G.F. Gribakin and M.Yu. Kuchiev, Phys. Rev. A **55**, 3760 (1997).
[54] W. Becker, S. Long, and J.K. McIver, Phys. Rev. A **41**, 4112 (1990); **50**, 1540 (1994).
[55] S. Flügge, *Practical Quantum Mechanics* (Springer-Verlag, Heidelberg, 1971), Vol. 1.